Alleles of the Yeast *PMS1* Mismatch-Repair Gene That Differentially Affect Recombination- and Replication-Related Processes

Caroline Welz-Voegele,* Jana E. Stone,† Phuoc T. Tran,‡ Hutton M. Kearney,† R. Michael Liskay,‡ Thomas D. Petes† and Sue Jinks-Robertson*,[1]

**Department of Biology, Emory University, Atlanta, Georgia 30322, †Department of Biology, Curriculum in Genetics and Molecular Biology, University of North Carolina, Chapel Hill, North Carolina 27599 and ‡Department of Molecular and Medical Genetics, Oregon Health and Science University, Portland, Oregon 97201*

Manuscript received March 27, 2002
Accepted for publication August 30, 2002

ABSTRACT

Mismatch-repair (MMR) systems promote eukaryotic genome stability by removing errors introduced during DNA replication and by inhibiting recombination between nonidentical sequences (spellchecker and antirecombination activities, respectively). Following a common mismatch-recognition step effected by MutS-homologous Msh proteins, homologs of the bacterial MutL ATPase (predominantly the Mlh1p-Pms1p heterodimer in yeast) couple mismatch recognition to the appropriate downstream processing steps. To examine whether the processing steps in the spellchecker and antirecombination pathways might differ, we mutagenized the yeast *PMS1* gene and screened for mitotic separation-of-function alleles. Two alleles affecting only the antirecombination function of Pms1p were identified, one of which changed an amino acid within the highly conserved ATPase domain. To more specifically address the role of ATP binding/hydrolysis in MMR-related processes, we examined mutations known to compromise the ATPase activity of Pms1p or Mlh1p with respect to the mitotic spellchecker and antirecombination activities and with respect to the repair of mismatches present in meiotic recombination intermediates. The results of these analyses confirm a differential requirement for the Pms1p ATPase activity in replication *vs.* recombination processes, while demonstrating that the Mlh1p ATPase activity is important for all examined MMR-related functions.

MISMATCH-repair (MMR) systems promote genome stability by detecting and dealing with distortions in the DNA double helix (reviewed in Harfe and Jinks-Robertson 2000a). These systems are best known for their role in removing mispaired or extrahelical nucleotides generated during DNA replication ("spellchecker" function), with defects resulting in a strong mutator phenotype. In addition to their replication-editing function, MMR systems also detect mismatches in the heteroduplex recombination intermediates that involve the pairing of single strands derived from different duplex DNA molecules. Detection of recombination-associated mismatches triggers either a repair process that restores perfect base complementarity or an antirecombination activity that prevents the recombination event from going to completion. Finally, MMR systems in some organisms are important for detecting DNA damage and for triggering appropriate cell-cycle arrest or apoptotic responses.

The MMR system of *Escherichia coli* contains three dedicated "Mut" proteins and has served as a paradigm for the more complicated MMR systems of eukaryotic organisms (reviewed in Modrich and Lahue 1996). MMR in *E. coli* is initiated when a homodimer of the MutS protein binds mismatches. A MutL homodimer then couples the MutS-dependent mismatch recognition to downstream processing steps by activating the latent endonuclease activity of the MutH protein. MutH specifically nicks the nascent strand to initiate its removal by a helicase and one or more exonucleases, and the resulting gap is filled in by DNA polymerase and sealed by ligase to complete the repair process. In eukaryotes there are multiple MutS and MutL homologs (Msh and Mlh proteins, respectively) that are involved in MMR processes, but no known MutH homologs (reviewed in Harfe and Jinks-Robertson 2000a). The active forms of the eukaryotic Msh and Mlh proteins are heterodimers instead of homodimers, with the heterodimers generally having distinct but overlapping functions in MMR. The recently solved crystal structures of bacterial MutS homodimers have revealed that they are, in fact, structural heterodimers (Lamers *et al.* 2000; Obmolova *et al.* 2000), which can account for the existence of heterodimers rather than homodimers in eukaryotes. In the yeast *Saccharomyces cerevisiae*, mismatches in nuclear DNA are recognized by either an Msh2p-Msh3p or an Msh2p-Msh6p heterodimer (Johnson *et al.* 1996b; Marsischky *et al.* 1996), which then interacts with a MutL-like heterodimer composed of Mlh1p complexed with Pms1p, Mlh2p, or Mlh3p (Wang *et al.* 1999). As the Mlh1p-

[1]*Corresponding author:* Department of Biology, 1510 Clifton Rd., Emory University, Atlanta, GA 30322. E-mail: jinks@biology.emory.edu

Mlh2p and Mlh1p-Mlh3p heterodimers play only minor roles in the repair of replication errors (Flores-Rozas and Kolodner 1998; Harfe *et al.* 2000) and have no reported antirecombination activity, only the Mlh1p-Pms1p heterodimer will be considered here.

Functionally important regions of the yeast Mlh1 and Pms1 proteins have been deduced by aligning MutL homologs from diverse organisms (Ban and Yang 1998; Crouse 1998) and by mutational analyses (Pang *et al.* 1997; Tran and Liskay 2000). Protein alignments have revealed a highly conserved region at the amino terminus that contains the four domains characteristic of the GHL (*g*yrase b, *H*sp90, and Mut*L*) family of ATPases (Dutta and Inouye 2000). Functionally important conformational changes in the N-terminal regions of GHL family proteins are associated with ATP binding and hydrolysis, with the N-terminal ends of MutL, and with gyrase b homodimerizing upon ATP binding (Wigley *et al.* 1991; Ali *et al.* 1993; Prodromou *et al.* 1997a,b; Ban and Yang 1998; Grenert *et al.* 1999). Studies with mutant Mlh1 and Pms1 proteins support a comparable amino-terminal heterodimerization cycle associated with ATP binding and hydrolysis (Tran and Liskay 2000). In addition, genetic studies have revealed an ATP-related asymmetry between the yeast Mlh1p and Pms1p subunits in terms of their contributions to the spellchecker function of the complex (Tran and Liskay 2000). Although Mlh1p and Pms1p share little amino acid similarity outside of the highly conserved N terminus, the C-terminal 200–300 amino acids of each protein are necessary and sufficient for ATP-independent heterodimer formation and are required for the spellchecker function of the complex (Pang *et al.* 1997). Finally, the C-terminal 13 amino acids of yeast Mlh1p are identical to the C-terminal 13 amino acids of human MLH1, but this highly conserved motif is not present in Pms1p. This carboxy-terminal homology (CTH) motif of Mlh1p is not required for interaction with Pms1p in two-hybrid assays, but is required for spellchecker function (Pang *et al.* 1997).

The repair of mismatches in heteroduplex recombination intermediates can result in the replacement of one allele with the sequence of another allele ("gene conversion"), which is manifested in meiosis as the non-Mendelian segregation of allelic sequences. If mismatches in meiotic recombination intermediates are not repaired, segregation of the corresponding alleles at the next round of DNA replication will result in genetically different daughter cells (postmeiotic segregation, or PMS). In yeast, gene conversion is much more common than PMS, indicating that most mismatches are efficiently recognized and repaired by the MMR machinery (Petes *et al.* 1991). Although it is not known what triggers the repair *vs.* antirecombination activity of MMR systems, the antirecombination activity effectively limits recombination between nonidentical ("homeologous") sequences, thereby reducing genome rearrangements and enforcing species barriers (reviewed in Harfe and Jinks-Robertson 2000a,b). In *S. cerevisiae*, mitotic recombination is exquisitely sensitive to potential mismatches, with a single nonidentity between 350-bp recombination substrates being sufficient to reduce the rate of recombination in a MMR-dependent manner (Datta *et al.* 1997). Although elimination of yeast Msh2p, Mlh1p, or Pms1p results in identical mutator phenotypes, the antirecombination activity of Msh2p is consistently greater than that of Pms1p or Mlh1p (Chen and Jinks-Robertson 1999; Nicholson *et al.* 2000). In addition, the Sgs1p helicase appears to be redundant with MMR-associated antirecombination (Myung *et al.* 2001), but has no known role in the repair of DNA mismatches.

The genetic differences between the MMR-associated spellchecker and antirecombination activities in yeast suggest that the Mlh1p-Pms1p-dependent steps downstream of mismatch recognition may be different during DNA replication *vs.* recombination. In addition, the ATPase-related functional asymmetry observed in the spellchecker functions of Mlh1p and Pms1p may extend to the recombination-related activities of the proteins as well. These issues are addressed in the current study by (1) identifying "separation-of-function" alleles of *PMS1* that partially uncouple the mitotic spellchecker and antirecombination functions, (2) examining the mitotic antirecombination effects of known mutations in *MLH1* or *PMS1* that compromise ATP binding or hydrolysis, and (3) examining the effects of eliminating Mlh1p or Pms1p ATP hydrolysis activity on the repair of mismatches in meiotic recombination intermediates.

MATERIALS AND METHODS

Media and growth conditions: Strains were grown vegetatively at 30° and sporulated at 18°; a complete list of yeast strains is given in Table 1. Standard media and genetic techniques were used for mitotic growth, sporulation, and tetrad dissection (Sherman 1991), except as noted below. Strains were grown nonselectively in YEP medium containing either 2% glycerol and 2% ethanol (YEPGE) or 2% dextrose (YEPD). Each liter of YEPGE and YEPD was supplemented with 500 mg adenine hemi-sulfate (Sigma, St. Louis) to avoid adenine limitation during nonselective growth. For selection of yeast transformants that had incorporated the *kan* marker, each liter of YEPD was supplemented with 200 mg of Geneticin (Sigma).

Synthetic dextrose (SD) medium was supplemented with all but the one amino acid or base needed for selective growth (*e.g.*, SD-His is deficient in histidine). Additional tryptophan (30 μg/ml) was added to the SD media as well as to the YEP media for growth of strains containing the *trp5*Δ allele (*i.e.*, SJR1392 and its derivatives). Canavanine-resistant (Can-R) mutants were selected on SD-Arg medium supplemented with L-canavanine sulfate to a concentration of 60 μg/ml (SD-Arg + Can). Ura$^-$ segregants were selected on SD plates supplemented with required amino acids and containing 0.1% 5-fluoroorotic acid (5-FOA; Boeke *et al.* 1984). For the selection of His$^+$ mitotic recombinants, dextrose in the SD medium was replaced with 2% glycerol, 2% ethanol, and 2% galactose (SGGE-His).

TABLE 1

Yeast strains

Strain[a]	Description	Source of construction
SJR1294	Used to screen for separation-of-function *pms1* alleles	This study
SJR1392	Contains homologous (*LYS2*) and homeologous (*HIS3*) recombination substrates	This study
SJR1470	SJR1392 *mlh1Δ::URA3*	This study
SJR1471	SJR1392 *pms1Δ*	This study
SJR1528	SJR1392 *mlh1-E31A*	This study
SJR1529	SJR1392 *mlh1-G98A*	This study
SJR1530	SJR1392 *pms1-E61A*	This study
SJR1531	SJR1392 *pms1-G128A*	This study
SJR1532	SJR1392 *pms1-L124S*	This study
SJR1533	SJR1392 *pms1-I854M*	This study
SJR1561	SJR1392 *mlh1-G98A pms1-G128A*	This study
SJR1578	SJR1392 *mlh1-757stop*	This study
SJR1789	SJR1392 *pms1-E61A,I854M*	This study
SJR1790	SJR1392 *pms1-G128A,I854M*	This study
PD73	*his4-AAG* haploid used to construct diploids for meiotic analyses	Detloff *et al.* (1991)
HMY91	PD73 *mlh1Δ::kanMX4*	This study
HM94	PD73 *mlh1Δ::URA3*	This study
HM92	PD73 *pms1Δ::kanMX4*	This study
DB10	PD73 *pms*1Δ	This study
JSY88	PD73 *mlh1-E31A*	This study
JSY116	PD73 *pms1-E61A*	This study
AS4	*HIS4* haploid used to construct diploids for meiotic analyses	Stapleton and Petes (1991)
DTK318	AS4 *mlh1Δ::URA3*	This study
DNY95	AS4 *pms1Δ*	This study
JSY89	AS4 *mlh1-E31A*	This study
JSY117	AS4 *pms1-E61A*	This study
PD83	*his4-AAG/HIS4*	PD73 × AS4 (Detloff *et al.* 1991)
HMY95	*his4-AAG/HIS4 mlh1Δ::kanMX4/mlh1Δ::URA3*	HMY91 × DTK318
DB101	*his4-AAG/HIS4 mlh1Δ::URA3/mlh1Δ::URA3*	HMY94 × DTK318
HMY96	*his4-AAG/HIS4 pms1Δ::kanMX4/pms1Δ*	HMY92 × DNY95
DB100	*his4-AAG/HIS4 pms1Δ/pms1Δ*	DB10 × DNY95
JSY76	*his4-AAG/HIS4 mlh1-E31A/mlh1-E31A*	JSY88 × JSY89
JSY80	*his4-AAG/HIS4 pms1-E61A/pms1-E61A*	JSY116 × JSY117
JSY106	*ARG4* derivative of AS4 for measuring Can-R rate	This study
JSY108	AS4 *ARG4 mlh1Δ::URA3*	This study
JSY104	AS4 *ARG4 mlh1-E31A*	This study
JSY107	AS4 *ARG4 pms1Δ*	This study
JSY105	AS4 *ARG4 pms1-E61A*	This study

[a] SJR1294, *MATα ade2-101$_{oc}$ his3Δ200 ura3(Nhe)-[HIS3::intron::cβ2(94%)]-ura3(Nhe) lys2ΔRV::hisG leu2-R pGAL-PMS1*; SJR1392, *MATα ade2-101$_{oc}$ his3Δ200 lys2ΔRV::hisG trp5Δ::kan ura3(Nhe)-[HIS3::intron::cβ2/cβ7(91%)]-ura3(Nhe) leu2(K)-[lys2Δ3′-lys2Δ5′]-LEU2*; AS4, *MATα trp1 arg4 tyr7 ade6 ura3*; PD73, *MAT***a** *leu2 ade6 ura3 his4-AAG*.

Sporulation of diploid cells and tetrad dissection were performed as described by Fan *et al.* (1995). For meiotic analyses, purified diploids were not used, since diploids homozygous for *pms1* or *mlh1* rapidly accumulate recessive lethal mutations. Instead, haploid parents were mated overnight on YEPD plates and then were immediately transferred to sporulation plates. Tetrads were dissected on YEPD medium and the resulting spore clones were directly replica plated to appropriate selective media. Sectored His^+/His^- colonies were scored by light microscopy.

Yeast strains used for mitotic studies: Strain SJR1294 was used as a host to identify plasmid-encoded *pms1* alleles conferring mutator and/or hyperrecombination phenotypes. The mutator phenotype was assessed by forward mutation to canavanine resistance, while the recombination phenotype was assessed using 94%-identical *HIS3::intron::cβ2* inverted-repeat (IR) substrates (see Datta *et al.* 1997). In preliminary experiments, we found that the high chromosomal mutation rate of a *pms1*Δ host strain interfered with the efficient detection of plasmid-encoded *pms1* alleles. To circumvent this problem, the endogenous *PMS1* promoter was replaced with the *GAL1* promoter by transforming cells with a PCR fragment generated using plasmid pFA6a-kanMX6-PGAL1 (Longtime *et al.* 1998) as a template. The presence of the resulting galactose-regulated *PMS1* allele (*pGAL-PMS1*) resulted in strong mutator and hyper-recombination phenotypes only when cells were grown in the absence of galactose.

Strain SJR1392 contains both homeologous (92% identical) and homologous (100% identical) IR recombination substrates. This strain was constructed by targeting plasmids containing

homeologous *HIS3::intron::cβ2/cβ7* substrates (pSR303) and homologous *LYS2* substrates (pRS304) to the *URA3* and *LEU2* loci, respectively. Transformants containing a single copy of each plasmid were identified by Southern analysis. Ura$^-$ segregants were selected on 5-FOA medium, and retention of the homeologous recombination substrates was confirmed by the ability to produce His$^+$ recombinants.

An *mlh1Δ::URA3* allele was introduced into SJR1392 by transformation with *Sac*I/*Bam*HI-digested *ymlh1::URA3* (Prolla *et al.* 1994). *Bst*XI-digested pJH523 (Kramer *et al.* 1989) was used in a two-step allele replacement procedure to introduce a *pms1Δ* allele. All *mlh1Δ* and *pms1Δ* strains were verified by PCR or Southern analysis. Derivatives containing point mutations in *PMS1* or *MLH1* were constructed by two-step allele replacement, and the presence of the mutation of interest was confirmed by genomic DNA sequencing. Plasmids pYI-mlh1-31, pYI-mlh1-98, pYI-pms1-61 TV II, and pYI-pms1-128 TV II were used to introduce the *mlh1-E31A*, *mlh1-G98A*, *pms1-E61A*, and *pms1-G128A* alleles, respectively (for details see Tran and Liskay 2000). The *pms1-L124S*, *pms1-I854M*, and *mlh1-757stop* alleles were introduced using plasmids pSR759, pSR760, and pSR746, respectively (see below).

Strains used for meiotic recombination studies: Diploid strains used for meiotic recombination experiments were constructed by mating isogenic derivatives of the *HIS4* strain AS4 (Stapleton and Petes 1991) and the *his4-AAG* strain PD73 (Detloff *et al.* 1991). All diploids thus are heterozygous for the *his4-AAG* mutant allele, which has a single-base-pair change at the second position of the *HIS4* start codon. Haploid derivatives containing an *mlh1Δ::URA*, *pms1Δ*, *mlh1-E31A*, or *pms1-E61A* allele were constructed by transformation as described above for SJR1392. The *mlh1Δ::kanMX4* and *pms1Δ::kanMX4* alleles were introduced by transformation with PCR deletion cassettes generated using pFA6-*kanMX4* (Wach *et al.* 1994) as a template. To determine forward mutation rates at the *CAN1* locus, *ARG4* derivatives of haploid strains with the AS4 genetic background were constructed by transformation with *Age*I-digested pMW52 (White *et al.* 1993).

Plasmids: Plasmid pSR303 contains the *HIS3::intron::cβ2/cβ7* homeologous recombination substrates and was constructed by combining 5′ cβ2 and 3′ cβ7 recombination cassettes as inverted repeats (Figure 1A). Plasmid pSR266 contains a full-length *HIS3::intron* gene, with a unique *Bam*HI site within the intron, and was used to generate both the 5′ and 3′ cassettes (see Datta *et al.* 1996). Plasmids pSR273 and pSR301 were constructed by inserting an 800-bp *Bam*HI/*Bgl*II cβ2 and a 783-bp *Bam*HI/*Bgl*II cβ7 fragment, respectively, into the *Bam*HI site of plasmid pSR266. The cβ7 3′ cassette plasmid pSR302 was derived from pSR301 by deleting the *Sal*I fragment upstream of the cβ7 sequences (*i.e.*, the 5′ portion of *HIS3* and the 5′ part of the intron). A *Sma*I fragment containing the 5′ cβ2 cassette (from pSR273) was then inserted into the filled-in *Spe*I site of pSR302 in reverse orientation relative to the 3′ cβ7 cassette.

Plasmid pSR304 contains the *lys2Δ5′* and *lys2Δ3′* homologous recombination substrates oriented as IRs (Figure 1B) and was constructed using *LYS2* sequences derived from pDP6 (Fleig *et al.* 1986). First, a 2.7-kb *Hinc*II/*Hin*dIII fragment containing the 3′ end of *LYS2* (*lys2Δ5′* allele) was directionally cloned into *Sma*I/*Hin*dIII-digested pRS305 (Sikorski and Hieter 1989), yielding plasmid pSR300. A 3-kb *Xba*I/*Stu*I fragment containing the 5′ end of *LYS2* (*lys2Δ3′* allele) was then inserted into *Xba*I/*Sst*I (blunt)-digested pSR300, with the resulting plasmid (pSR304) containing the *lys2Δ5′* allele downstream of and in inverted orientation relative to the *lys2Δ3′* allele. The region of overlap between the *lys2Δ5′* and *lys2Δ3′* alleles is ~900 bp.

Plasmid pSR758 contains the 2715-bp *PMS1* open reading frame and was constructed by cloning a 4-kb chromosomal *Bgl*II/*Sal*I fragment (from YIp5-PMS1; obtained from D. Maloney) into *Bam*HI/*Sal*I-digested pRS315 (LEU2-CEN vector; Sikorski and Hieter 1989). pSR758 was the source for the *PMS1* fragments that comprise the three deletion plasmids used in gap-repair experiments. pRS315-PMS1Δ1 (pSR764) has a deletion of the first 590 bp of the *PMS1* coding sequence between the *Mlu*I and *Hin*P1I sites at −33 and +591, respectively, relative to the start codon; pRS315-PMS1Δ2 (pSR765) has a centrally located 1090-bp deletion extending from the *Eco*0109I site at +387 to the *Fok*I site at +1477; and pRS315-PMS1Δ3 (pSR766) has a 927-bp deletion encompassing the C-terminal region of *PMS1*, extending from the *Bsp*HI site at +1713 to the *Nco*I site at +2640. Each of the three deletion plasmids contains a unique *Bam*HI site between the *PMS1* fragments that flank the deleted segment.

pSR761 contains the *MLH1* locus and was derived by inserting a 7-kb chromosomal *Sac*I fragment (from YEp24-MLH1; Prolla *et al.* 1994) into pRS306 (Sikorski and Hieter 1989). The *mlh1-757stop* allele (pSR746) was constructed by replacing codon 757 of the *MLH1* coding sequence with a TAG stop codon using the QuikChange site-directed mutagenesis kit (Stratagene, La Jolla, CA). The resulting mutation was confirmed by DNA sequencing.

Random mutagenesis of the *PMS1* coding sequence and incorporation of mutations by gap repair: Appropriate *PMS1* fragments were generated by mutagenic PCR and were then recombined *in vivo* into plasmids pRS315-PMS1Δ1, pRS315-PMS1Δ2, or pRS315-PMS1Δ3 using a standard yeast gap-repair procedure (Muhlrad *et al.* 1992). *Taq* DNA polymerase was used for the PCR mutagenesis; the error frequency of the enzyme was increased by doubling the concentration of dATP or dGTP relative to the other dNTP's and by increasing the $MgCl_2$ concentration to 3 mm. Plasmids for the *in vivo* gap repair were prepared by digestion with *Bam*HI, followed by treatment with shrimp alkaline phosphatase. Gap repair of pRS315-PMS1Δ1 was accomplished using a 687-bp PCR fragment extending from −61 to +626 of the *PMS1* sequence; gap repair of plasmid pRS315-PMS1Δ2 was effected using an 1167-bp PCR fragment extending from +349 to +1516 of the *PMS1* sequence; and gap repair of pRS315-PMS1Δ3 was done using a 1029-bp PCR fragment extending from +1668 to +2697 of the *PMS1* sequence.

Strain SJR1294 was cotransformed with 1 μg of purified PCR fragment and 0.1 μg of gapped vector, and transformants were selected on SD-Leu medium. Control experiments with gapped vector only indicated a gap-repair efficiency of >95%. Approximately 1000 transformants derived from each of the three gap-repair reactions were selectively purified. Transformants were patched onto SD-Arg + Can or SGGE-His medium to score mutation or homeologous recombination frequency, respectively. Approximately 30% of the transformants exhibited phenotypes characteristic of a *pms1Δ* strain and were assumed to contain plasmid-encoded null alleles. Plasmid DNA was isolated from those transformants that consistently exhibited a separation-of-function phenotype (either a mutator or a hyper-rec phenotype, but not both phenotypes) and was used to retransform SJR1294. Following the confirmation of a separation-of-function phenotype, the relevant portion of the mutagenized *pms1* allele was sequenced. The separation-of-function alleles *pms1-L124S* and *pms1-I854M* were identified in this manner. For integration into the yeast genome, the *pms1-L124S* and *pms1-I854M* alleles were transferred to the integrating vector pRS306 (Sikorski and Hieter 1989) as *Sac*II/*Kpn*I fragments, yielding plasmids pSR759 and pSR760, respectively.

Two-hybrid assays: Plasmids used in two-hybrid assays were constructed by inserting the coding sequences of wild-type

Pms1p and Mlh1p into vectors pGAD424 (Bartel *et al.* 1993) and pBTM116 (Vojtek *et al.* 1993), respectively. pGAD424 and pBTM116 contain the Gal4p activation and the LexA DNA-binding domains, respectively. The pGAD-*PMS1* construct was mutagenized to yield pGAD-*pms1-I854M* using the QuikChange site-directed mutagenesis kit (Stratagene). Interactions of proteins were assessed by cotransforming pGAD and pBT derivatives into yeast strain L40, which contains both *lacZ* and *HIS3* reporter constructs (Vojtek *et al.* 1993). β-Galactosidase activity was measured in liquid assays as described previously (Pang *et al.* 1997).

Rate measurements and statistical analyses: The method of the median (Lea and Coulson 1949) was used to calculate mutation and recombination rates. Data from at least 16 independent cultures (typically 8 cultures from each of two independent isolates) were used for each rate determination. For the experimentally derived medians, 95% confidence intervals (CIs) were determined (Dixon and Massey 1969) and these were then used to calculate 95% CIs for the corresponding rates. For rate determinations using SJR1392 and its derivatives, individual colonies were inoculated into 5 ml YEPGE medium and grown for 3 days on a roller drum. Cells were harvested by centrifugation, washed with H_2O, and resuspended in 1 ml H_2O. Aliquots of appropriate dilutions were plated on SD-Arg + Can to select Can-R mutants, on SD-His to select His^+ (homeologous) recombinants, on SD-Lys to select Lys^+ (homologous) recombinants, and on YEPD to determine the number of viable cells. Plates were incubated for 2 days (YEPD, SD-Arg + Can, SD-Lys) or 4 days (SGGE-His) before counting colonies. Mutation rates to Can-R in AS4 and PD73 and in their derivatives were similarly determined, except that cultures were grown overnight in YEPD before selective plating, total viable cells were determined by plating on SD-Arg, and colonies arising on SD-Arg + Can were counted after 3 days. Comparisons of the distributions of meiotic spore classes derived from different diploids were made by Fisher's exact test with two-tailed *P* values. Results were considered significant if $P < 0.05$.

RESULTS

Mutagenesis of *PMS1* and identification of mitotic separation-of-function mutations: A *PMS1* gene contained on a *CEN* vector was randomly mutagenized and the resulting alleles were screened for a mitotic separation-of-function phenotype in a strain devoid of the wild-type Pms1 protein (see materials and methods for details of the mutagenesis). Specifically, transformants containing the mutagenized plasmids were screened for an associated increase in either the spontaneous mutation or the homeologous recombination frequency, but not both. The mutator phenotype was assessed by replica plating transformants to canavanine medium, which selectively identifies forward mutations at the *CAN1* locus (Can-R mutants). The level of homeologous recombination was assessed by replica plating transformants to histidine-deficient medium, which selects for inversion events that reconstitute a full-length *HIS3::intron* gene (Figure 1A). All candidate separation-of-function plasmids identified in the screen conferred little or no mutator phenotype, but resulted in a clearly elevated level of homeologous recombination. No candidates with the opposite phenotype were identified.

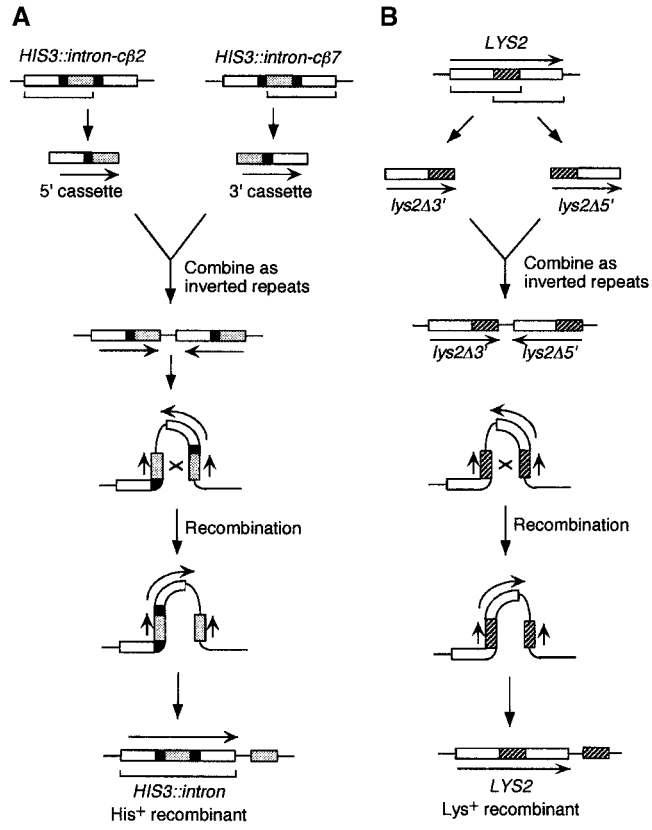

Figure 1.—Homeologous and homologous inverted-repeat recombination substrates. (A) Homeologous substrates. The 5′ cβ2 cassette consists of the 5′ portion of the *HIS3* coding sequence, the 5′ portion of the intron, and the cβ2 cDNA sequences, whereas the 3′ cassette is composed of cβ7 cDNA sequences, the 3′ portion of the intron, and the 3′ portion of the *HIS3* coding sequence. Open boxes correspond to *HIS3* coding sequences, solid boxes to intron sequences, and the cross-hatched boxes to the cβ2 and cβ7 recombination substrates (~800 bp of homology with 92% sequence identity). (B) Homologous substrates. The hatched box within the *LYS2* gene corresponds to the ~900 bp of perfect identity between the *lys2Δ5′* and *lys2Δ3′* recombination substrates. In both A and B, selection of prototrophic colonies identifies recombination events that reorient the region between the inverted-repeat recombination substrates. Reorientation can occur by a crossover event, by unequal sister chromatid gene conversion (Chen and Jinks-Robertson 1998), or by a combination of break-induced replication and single-strand annealing (Bartsch *et al.* 2000).

To confirm that the elevated recombination conferred by the putative *pms1* separation-of-function alleles was specific for homeologous substrates, the plasmid-encoded alleles were introduced into the *PMS1* locus of strain SJR1392, which contains identical ("homologous") *LYS2* recombination substrates as well as the homeologous *HIS3::intron* substrates. The *LYS2*-based homologous system (Figure 1B) is composed of inverted repeats and thus is comparable in structure to the homeologous *HIS3::intron* system. As with the *HIS3::intron* system, replication between the *lys2* inverted repeats reorients the region between them, resulting in a full-

TABLE 2

Mutation and recombination rates in wild-type and *pms1* strains

Genotype[a]	Mutation rate ($\times 10^{-7}$)[b]	Mutation rate relative to WT	Recombination rate ($\times 10^{-6}$)[b]		His^+/Lys^+ rate[c]	His^+/Lys^+ rate relative to WT
			Homologous (Lys^+)	Homeologous (His^+)		
Wild type	1.19 (1.12–1.56)	1.0	3.32 (2.66–4.33)	0.0576 (0.0542–0.0742)	0.017	1.0
*pms1*Δ	71.1* (52.6–87.2)	60	3.85 (3.07–5.25)	0.725* (0.549–0.885)	0.19	11
pms1-L124S	1.55 (1.25–2.25)	1.3	2.33 (1.75–2.83)	0.171* (0.142–0.228)	0.073	4.2
pms1-I854M	1.48 (1.24–1.68)	1.2	2.96 (2.29–3.49)	0.132* (0.103–0.164)	0.046	2.7
pms1-E61A	1.65 (1.43–2.25)	1.4	3.54 (3.09–4.58)	0.172* (0.129–0.244)	0.049	2.8
pms1-G128A	1.29 (1.18–1.63)	1.1	2.62 (2.29–3.57)	0.174* (0.146–0.227)	0.066	3.8
pms1-E61A,I854M	5.47* (4.87–7.15)	4.6	2.53 (1.87–2.94)	0.337* (0.298–0.429)	0.16	9.4
pms1-G128A,I854M	7.18* (5.82–8.28)	6.0	2.03* (1.72–2.37)	0.318* (0.260–0.403)	0.19	11

WT, wild type. *Significantly different from the rate in the wild-type control strain.

[a] All strains are isogenic derivatives of SJR1392.

[b] Ninety-five percent confidence intervals are indicated in parentheses.

[c] The His^+/Lys^+ rate corresponds to the average rate ratio for the independent cultures examined. The His^+/Lys^+ rate ratio for each independent culture was obtained by dividing the His^+ rate by the Lys^+ rate for that particular culture. The His^+ or Lys^+ rate calculation for an individual culture was determined by using the number of prototrophic colonies as the median (Lea and Coulson 1949).

length *LYS2* gene whose presence can be identified on lysine-deficient medium.

As shown in Table 2, elimination of Pms1p in the SJR1392 strain background resulted in a 60-fold increase in the rate of Can-R mutants. When normalized to the homologous recombination rate, the increase in the homeologous recombination rate was 11-fold in the *pms1*Δ mutant relative to the *PMS1* strain; similarly, normalized rates are used when describing homeologous recombination in *pms1* (or *mlh1*) missense mutants. Quantitation of recombination and mutation rates in the *pms1* mutants identified in the screen confirmed only two separation-of-function *pms1* alleles. Each allele resulted in a significant (3- to 4-fold) increase in the homeologous recombination rate, but no significant increase in the forward mutation rate at the *CAN1* locus (Table 2). DNA sequence analysis of the separation-of-function alleles revealed a mutation resulting in a leucine-to-serine change at amino acid 124 in one mutant (*pms1-L124S* allele) and a mutation causing an isoleucine-to-methionine change at amino acid 854 in the other mutant (*pms1-I854M* allele).

Pms1p-I854M interacts normally with Mlh1p in two-hybrid assays: The *pms1-I854M* allele alters a single amino acid in the C-terminal region of Pms1p, a region that is essential for interaction with Mlh1p in two-hybrid assays (Figure 2; Pang *et al.* 1997). One possible explanation for the separation-of-function phenotype conferred by the *pms1-I854M* allele is that more of the Mlh1p-Pms1p complex is needed to regulate mitotic recombination than is needed to correct DNA replication errors. A decrease in the amount/stability of the complex would thus be expected to elevate homeologous recombination rates to a greater extent than mutation rates. To determine whether the I854M change significantly affects the level of the Pms1p-Mlh1p complex *in vivo*, we used two-hybrid assays to compare the interaction of Mlh1p with the wild-type *vs.* the I854M mutant Pms1 protein. As shown in Figure 3, the interactions were indistinguishable in a qualitative phenotypic assay as well as in a quantitative β-galactosidase assay, suggesting that the I854M change affects neither the stability of Pms1p nor its interaction with Mlh1p.

Role of Pms1p ATP binding/hydrolysis in mitotic MMR functions: The L124S change is immediately adjacent to conserved motif III of the GHL family of ATPases, which is important in ATP binding and/or associated conformational changes (Ban *et al.* 1999; see Figure 2). The identification of the *pms1-L124S* allele in the separation-of-function screen suggested that ATP binding/hydrolysis by Pms1p might be more important for its antirecombination activity than for its spellchecker function. To pursue this further, we introduced the *pms1-G128A* and *pms1-E61A* alleles, which are predicted to compromise ATP binding (and/or associated conformational changes) and hydrolysis, respectively, into the SJR1392 strain background. These alleles were previously reported to have little, if any, effect on the spellchecker functions of the corresponding proteins in the *CAN1* mutation assay (Tran and Liskay 2000). The results obtained with the *pms1-E61A* and *pms1-G128A* alleles were indistinguishable from those obtained with the *psm1-L124S* allele. As shown in Table 2, there was no significant increase in the rate of Can-R colonies, but there was a significant (three- to fourfold) increase in the rate of homeologous recombination in the *pms1-E61A* and *pms1-G128A* strains.

The separation-of-function phenotype conferred by mutations in the N-terminal ATP binding/hydrolysis domains of Pms1p was very similar to that associated

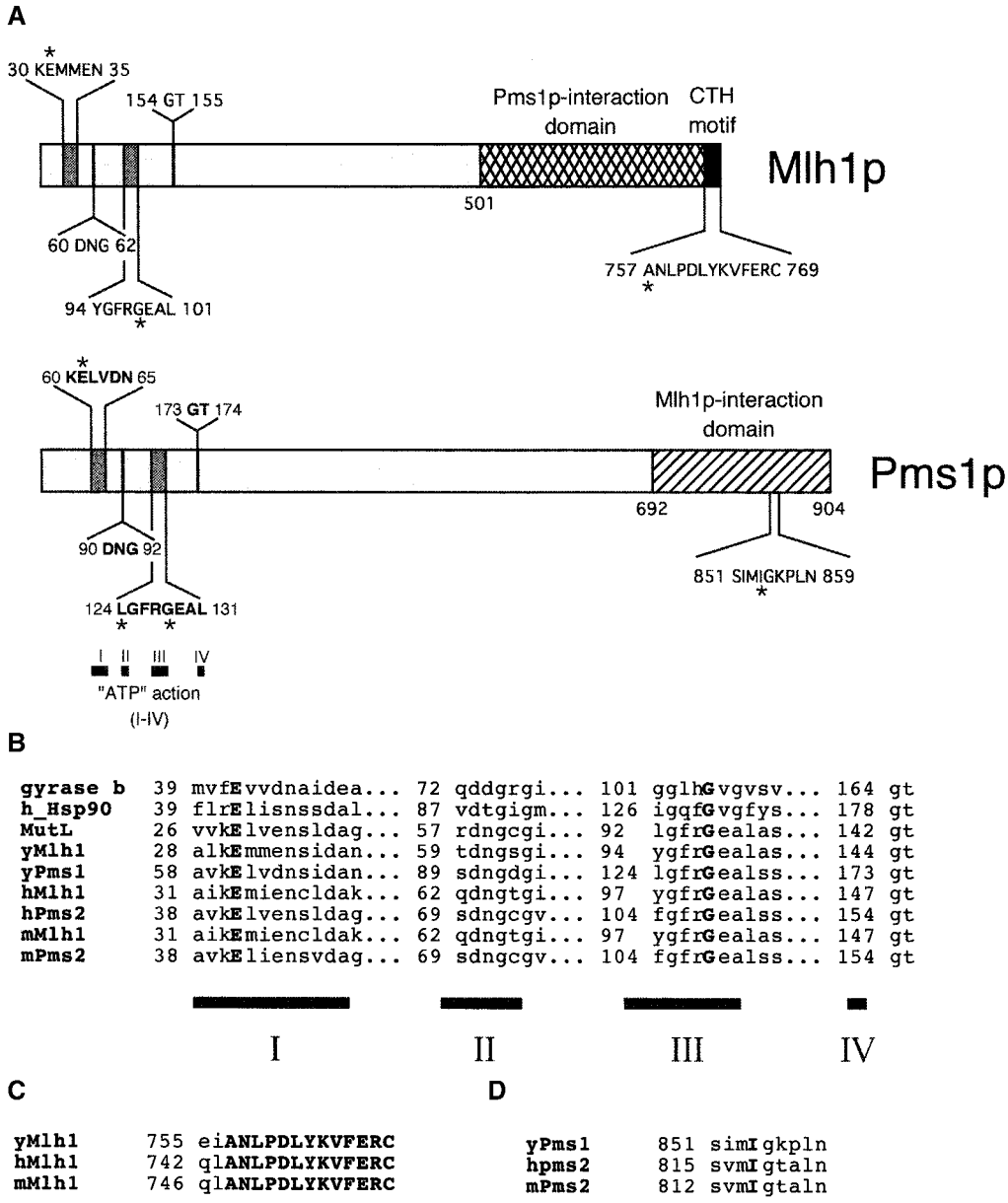

FIGURE 2.—Domains of Mlh1p and Pms1p. (A) Schematic representations of yeast Mlh1p and Pms1p are shown with specific motif sequences highlighted above or below each protein. Numbers correspond to the amino acid position in the protein. Asterisks denote residues that were mutated and examined as detailed in the text. (B) NH_2-terminal ATPase domains of GHL ATPases. ATPase motifs I–IV are designated by solid boxes and aligned sequences are shown above the motif boxes. Numbers correspond to the amino acid position of the first residue in the relevant motif. Conserved residues that were mutated in Mlh1p and/or Pms1p are shown in boldface type. (C) The CTH motifs of the yeast, human, and mouse Mlh1p orthologs are aligned and highlighted by boldface uppercase letters. (D) The COOH-terminal motif of yeast Pms1p that contains the *pms1-I854M* separation-of-function mutation. The yeast Pms1p I854 residue and the surrounding motif are present in the human and mouse orthologs.

with the C-terminal *pms1-I854M* allele. To determine whether the C- and N-terminal mutations affect Pms1p in fundamentally different ways, we constructed strains containing the double-mutant *pms1-E61A,I854M* or *pms1-G128A,I854M* allele. Both double-mutant strains exhibited significantly higher mutation and homeologous recombination rates than those observed with the corresponding single-mutant strains (Table 2), suggesting that the individual mutations have functionally distinct consequences. The mutator phenotype of the double mutants was very weak, however, with the mutation rates being 10-fold lower than that of an isogenic *pms1*Δ strain. In contrast, the ratio of homeologous to homologous recombination in the double mutants was similar to that in a *pms1*Δ strain. The double-mutant proteins thus retain most of their spellchecker activity, but appear to be completely defective for the mitotic antirecombination activity.

Role of Mlh1p ATP binding/hydrolysis in mitotic MMR functions: A functional asymmetry in the ATPase activities of Pms1p and Mlh1p has been demonstrated previously, with disruption of Mlh1p ATP binding/hydrolysis resulting in stronger mutator phenotypes than those resulting from comparable changes in Pms1p (TRAN and LISKAY 2000). We therefore examined the effects of the *mlh1-E31A* and *mlh1-G98A* alleles (direct counterparts of the *pms1-E61A* and *pms1-G128A* alleles, respectively; see Figure 2) on the mitotic spellchecker and antirecombination functions of the encoded mutant proteins (Table 3). In the SJR1392 strain background, deletion of *MLH1* resulted in a 53-fold elevation in the rate of forward mutation at *CAN1* and in a 9.7-

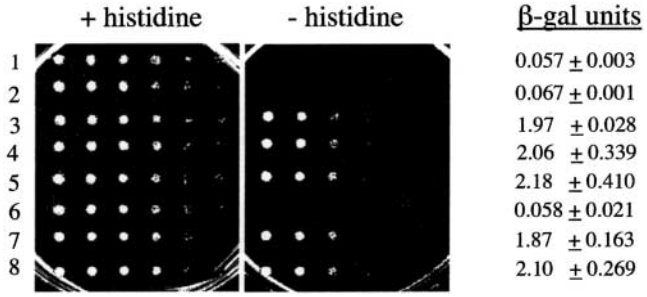

FIGURE 3.—Pms1-I854Mp interacts normally with Mlh1p in two-hybrid assays. Semiquantitative *HIS3* reporter assays were performed by serially diluting overnight cultures 1:5 and spotting cells using a 48-prong replicator onto minimal medium containing or lacking histidine. β-Glactosidase assays were performed two times with each strain; mean activity units and standard deviations are given. Row 1, pBT (vector) and pGAD-*PMS1*; row 2, pBT-*MLH1* and pGAD (vector); row 3, pBT-*MLH1* and pGAD-*PMS1*; rows 4–8, pBT-*MLH1* and pGAD-*pms1-I854M* clones 1–5. The pGAD-*pms1-I854M* clone in row 6 was found to have a nonsense mutation that truncated the protein after amino acid 865. On the basis of previous two-hybrid analyses (PANG *et al.* 1997), such a truncated protein would not be expected to interact with Mlh1p.

fold increase in the rate of homeologous (relative to homologous) recombination. These effects are statistically the same as those observed in the *pms1*Δ mutant. Both the *mlh1-E31A* and *mlh1-G98A* alleles were indistinguishable from the *mlh1*Δ allele in terms of the rate of His^+ recombinants, indicating that both ATP binding and hydrolysis are essential for the antirecombination activity of Mlh1p. In terms of the spellchecker function, the *mlh1-G98A* allele resulted in a 48-fold increase in the rate of Can-R colonies while the *mlh1-E31A* allele resulted in a lesser, 20-fold increase. In agreement with an earlier study (TRAN and LISKAY 2000), it thus appears that Mlh1p retains residual spellchecker activity when ATP hydrolysis, but not binding, is compromised. Finally, we constructed an *mlh1-G98A pms1-G128A* double-mutant strain. The spellchecker and antirecombination phenotypes of the double mutant were indistinguishable from those of an *mlh1*Δ or *pms1*Δ mutant.

Role of the Mlh1p CTH domain in mitotic MMR functions: The final 13 amino acids of yeast Mlh1p and human MLH1 are identical and constitute the CTH domain. This domain is not required for interaction between yeast Mlh1p and Pms1p in two-hybrid assays, but is required for the spellchecker function of the complex (PANG *et al.* 1997). To examine the role of the CTH domain in mitotic antirecombination, we replaced the codon specifying the first amino acid of the CTH domain with a stop codon (*mlh1-757stop* allele; see Figure 2). As shown in Table 3, the *mlh1-757stop* allele produced mutator and recombination phenotypes that were indistinguishable from those of a null (*mlh1*Δ) mutant.

Roles of Pms1p and Mlh1p ATP hydrolysis in the repair of mismatched meiotic recombination intermediates: In addition to the mitotic spellchecker and antirecombination activities, the yeast MMR system also detects and repairs the mismatch formed when a heterozygous marker (*e.g.*, alleles *A* and *a*) is included in a heteroduplex recombination intermediate. Efficient MMR is associated with high levels of gene conversion and low levels of PMS for heterozygous markers, and inefficient MMR results in low levels of conversion and high levels of PMS. PMS tetrads with two *A* spore colonies, one *a* spore colony, and one sectored *A*/*a* spore colony are called "5*A*:3*a*" tetrads whereas those with one *A* spore colony, two *a* spore colonies, and one sectored *A*/*a* colony are called "3*A*:5*a*" tetrads. Using this nomenclature (derived from eight-spored fungi), we define Mendelian segregation as 4*A*:4*a* and gene conversion events as 6*A*:2*a* or 2*A*:6*a*.

Diploid strains heterozygous for the *his4-AAG* muta-

TABLE 3

Mutation and recombination rates in wild-type and *mlh1* strains

Genotype[a]	Mutation rate ($\times 10^{-7}$)[b]	Mutation rate relative to WT	Recombination rate ($\times 10^{-6}$)[b]		His^+/Lys^+ rate[c]	His^+/Lys^+ rate relative to WT
			Homologous (Lys^+)	Homeologous (His^+)		
Wild type	1.19 (1.12–1.56)	1.0	3.32 (2.66–4.33)	0.0576 (0.0542–0.0742)	0.017	1.0
*mlh1*Δ	63.0* (52.6–98.1)	53	3.17 (2.71–5.61)	0.532* (0.348–0.775)	0.17	9.7
mlh1-E31A	23.5* (14.0–26.7)	20	3.35 (2.42–6.09)	0.528* (0.363–0.621)	0.16	9.1
mlh1-G98A	56.8* (41.2–79.6)	48	3.65 (2.85–4.86)	0.673* (0.498–0.815)	0.18	11
mlh1-G98A pms1-G128A	71.5* (53.9–87.5)	60	4.14 (2.98–5.35)	0.815* (0.247–1.07)	0.20	11
mlh1-757stop	69.2* (49.9–82.0)	58	4.43 (2.72–6.63)	0.815* (0.565–0.905)	0.18	11

*Significantly different from the rate in the wild-type control strain.

[a] All strains are isogenic derivatives of SJR1392.

[b] Ninety-five percent confidence intervals are indicated in parentheses.

[c] The His^+/Lys^+ rate corresponds to the average rate ratio for the independent cultures examined. The His^+/Lys^+ rate ratio for each independent culture was obtained by dividing the His^+ rate by the Lys^+ rate for that particular culture. The His^+ or Lys^+ rate calculation for an individual culture was determined by using the number of prototrophic colonies as the median (LEA and COULSON 1949).

TABLE 4

Rates of aberrant segregation at the *HIS4* locus in wild-type, *pms1*, and *mlh1* strains

Strain	Relevant genotype	Total tetrads	No. of tetrads/class						% ab.	% PMS/ab. tetrad[b]	% PMS/ab. spore[c]	Relative increase in PMS[d]
			4:4	6:2	2:6	5:3	3:5	Other ab.[a]				
PD83[e]	Wild type	482	202	73	108	22	21	56	58	18	18	1
HMY95/DB101[f]	*mlh1*Δ	465	199	18	16	83	70	79	57	85	89	4.9
JSY76	*mlh1-E31A*	388	154	24	42	52	45	71	60	62	69	3.8
HMY96/DB100[f]	*pms1*Δ	641	266	32	38	99	103	103	59	73	78	4.3
JSY80	*pms1-E61A*	358	150	45	42	33	29	59	58	35	40	2.2

ab., designates aberrant tetrads or spores.

[a] This class includes tetrads with two or more PMS and conversion events. The number of events (shown in parentheses for each class for each genotype):

wild type: ab. 4:4 (1), ab. 2:6 (1), deviant (dev.) 5:3 (1), 7:1 (3), 8:0 (11), 0:8 (16)
*mlh1*Δ: ab. 4:4 (13), ab. 6:2 (5), ab. 2:6 (4), dev. 5:3 (7), dev. 3:5 (5), dev. 4:4 (1), 7:1 (3), 8:0 (1)
mlh1-E31A: ab. 4:4 (12), ab. 6:2 (3), ab. 2:6 (1), dev. 5:3 (2), dev. 3:5 (2), 7:1 (4), 1:7 (4), 8:0 (1), 0:8 (3)
*pms1*Δ: ab. 4:4 (24), ab. 6:2 (5), ab. 2:6 (8), dev. 5:3 (5), dev. 3:5 (1), 7:1 (7), 1:7 (7), 8:0 (3), 0:8 (2)
pms1-E61A: ab. 4:4 (2), ab. 6:2 (2), ab. 2:6 (1), 7:1 (13), 1:7 (7), 8:0 (8), 0:8 (10).

[b] These percentages were calculated by dividing the total number of aberrant tetrads by the number of tetrads with one or more PMS event, excluding those that had both a PMS and a gene conversion event.

[c] These percentages were calculated (as described in the text) by dividing the number of sectored (PMS) spore colonies by the total number of PMS plus gene-conversion spore colonies.

[d] The percentage of PMS/aberrant spore colony values for each mutant strain were divided by the percentage of PMS/aberrant spore colony values observed in wild type.

[e] Although this strain was examined previously with purified diploids (Detloff *et al.* 1991), the data shown here include only diploids sporulated soon after mating.

[f] Data from these pairs of strains were not significantly different and were pooled.

tion in the *HIS4* start codon were used to analyze the effects of defects in Pms1p- or Mlh1p-associated ATP hydrolysis (*pms1-E61A* and *mlh1-E31A* alleles, respectively) on the repair of mismatches in heteroduplex recombination intermediates. The PD83 strain background was used in these experiments because of the very high level of meiotic recombination at *HIS4* (Nag *et al.* 1989), which occurs as a consequence of a high frequency of meiosis-specific double-strand breaks near the 5′ end of the gene (Fan *et al.* 1995). Depending on which DNA strand is transferred during heteroduplex formation, a heteroduplex composed of a wild-type strand and a strand with the *his4-AAG* substitution will contain either an A-A or a T-T mismatch (Detloff *et al.* 1991). As shown in Table 4, a strain with normal MMR (PD83) repaired both mismatches efficiently (Detloff *et al.* 1991), resulting in high levels of gene conversion and low levels of PMS.

In our previous studies, the efficiency of mismatch repair was determined by dividing the number of tetrads in which one or more spores exhibit PMS by the total number of tetrads with non-Mendelian (aberrant) segregation. This approach has two inherent problems. First, tetrads with multiple PMS or multiple conversion events are counted as equivalent to tetrads with a single PMS or conversion event. Second, it is not clear how to count a tetrad that contains both a conversion event *and* a PMS event. Consequently, here we used a different method to measure the efficiency of meiotic heteroduplex repair, which is based on counting the number of individual PMS and gene conversion spore *colonies* rather than *tetrads*. Using the definitions of tetrad classes given in Detloff *et al.* (1991), the number of PMS spore colonies (indicated in parentheses) counted in each class is the following: normal 4:4 (0), 6:2 (0), 2:6 (0), 5:3 (1), 3:5 (1), aberrant 4:4 (2), aberrant 6:2 (2), aberrant 2:6 (2), deviant 5:3 (3), deviant 3:5 (3), deviant 4:4 (4), 7:1 (1), 1:7 (1), 8:0 (0), and 0:8 (0). The number of gene conversion spore colonies counted for each class of tetrad is the following: normal 4:4 (0), 6:2 (1), 2:6 (1), 5:3 (0), 3:5 (0), aberrant 4:4 (0), aberrant 6:2 (0), aberrant 2:6 (0), deviant 5:3 (0), deviant 3:5 (0), deviant 4:4 (0), 7:1 (1), 1:7 (1), 8:0 (2), and 0:8 (2).

The tetrad/spore data for PD83 and mutant derivatives are presented in Table 4. The levels of aberrant segregation tetrads in all strains were similar, varying between 57 and 60%. As expected from previous studies (Williamson *et al.* 1985; Prolla *et al.* 1994), diploids homozygous for *mlh1*Δ or *pms1*Δ exhibited an increase in the relative frequencies of PMS spore colonies from 18% in wild type to 89 or 78%, respectively, indicating inefficient meiotic mismatch repair. Statistical comparison of the relative number of PMS *vs.* gene conversion spore colonies indicates that *mlh1*Δ strains had significantly less mismatch repair than the *pms1*Δ strains ($P < 0.0001$). Although the *mlh1-E31A* strain had significantly

TABLE 5

Genetic distances for intervals on chromosome *III* in wild-type and mutant strains

		HIS4-LEU2				*LEU2-CEN3*				*HIS4-CEN3*				*MAT-CEN3*				*HIS4-MAT*			
Strain	Genotype	P	N	T	cM	P	N	T	cM	P	N	T	cM	P	N	T	cM	P	N	T	cM
PD83	Wild type	118	1	73	21	204	182	82	9	53	50	91	23	97	85	166	24	47	14	78	58
HMY95	*mlh1*Δ	140	3	43	16*	191	187	79	9	58	67	72	18*	87	82	68	14*	56	4	42	32*
JSY76	*mlh1-E31A*	104	4	43	22	165	163	62	8	49	52	51	17*	87	73	112	21	45	6	56	43
HMY96	*pms1*Δ	161	1	89	19	264	270	93	7	70	69	100	21	93	75	124	21	47	8	80	47
JSY80	*pms1-E61A*	95	1	50	20	139	144	64	9	42	41	63	22	71	61	110	23	39	5	52	43

The numbers of tetrads in each class is shown, with P, N, and T indicating parental ditype, nonparental ditype, and tetratype tetrads, respectively. Only tetrads in which the flanking markers underwent Mendelian (4:4) segregation are included. Map distances for the *HIS4-LEU2* and *HIS4-MAT* intervals were calculated using the Perkins equation (Perkins 1949). Gene-centromere distances were calculated using the heterozygous centromere-linked *TRP1* marker as described by Sherman and Wakem (1991). For the gene-centromere intervals, the number of first-division segregation tetrads (P and N) and second-division segregation tetrads (T) were compared by Fisher's exact test. For the gene-gene intervals, the number of P, N, and T tetrads was compared using a 3×2 contingency chi-square test. *Significantly reduced ($P < 0.05$) map distance relative to the wild-type strain.

less MMR than the wild-type strain ($P < 0.0001$), it had significantly more repair than the *mlh1*Δ strain ($P < 0.0001$). Similarly, the *pms1-E61A* strain has less mismatch repair than the wild-type strain ($P < 0.002$), but more repair than the *pms1*Δ strain ($P < 0.0001$). Finally, relative to the corresponding null allele, the *pms1-E61A* allele did not appear to confer as severe a defect in meiotic MMR as the *mlh1-E31A* allele.

The frequency of PMS events at *HIS4* in the wild-type strain PD83 was higher than that observed in most studies involving different mutant alleles in other genetic backgrounds. Although one interpretation of this finding is that PD83 has a less efficient MMR system than that of other wild-type strains, we prefer a different explanation: that the efficiency of MMR is context dependent. One argument in support of this conclusion is based on an analysis of aberrant segregation of the heterozygous *arg4-17* allele in PD83. In 482 tetrads, we found 37 conversion events and no PMS events, a significant difference ($P < 0.002$) in the relative number of conversion and PMS tetrads compared to that observed for the *his4-AAG* marker. Since a heteroduplex formed between *arg4-17* and *ARG4* would contain either an A/A or a T/T mismatch (the same type of mismatch as expected for the *his4-AAG* marker), these results argue that the efficiency of meiotic MMR is affected by the context of the mismatch. In a previous study, Fogel *et al.* (1979) found that A/G or C/T mismatches failed to get repaired in a wild-type strain at frequencies (expressed as the percentage of PMS tetrads divided by total aberrant tetrads) of 12, 4, and 0% for mismatches located at the *HIS4*, *ARG4*, and *TRP1* loci, respectively.

Meiotic crossovers and spore viability in *pms1* and *mlh1* mutants: It has been observed previously that deletion of *MLH1*, but not *PMS1*, reduces crossovers in a variety of intervals (Hunter and Borts 1997; Wang *et al.* 1999). We calculated map distances for several genetic intervals on chromosome *III* in wild-type and mutant strains using only tetrads in which both markers for each interval underwent Mendelian segregation (Table 5). This analysis confirmed the previous observation that the *mlh1*Δ mutation significantly reduces crossovers in most genetic intervals examined (Hunter and Borts 1997; Wang *et al.* 1999). In contrast, the *mlh1-E31A* mutation significantly reduced crossovers only in the *HIS4-CEN3* interval. The difference in tetrad classes for the *mlh1*Δ compared to the *mlh1-E31A* strain was significant only for the *MAT-CEN3* interval. Neither the *pms1*Δ nor the *pms1-E61A* mutation significantly affected crossovers in any of the intervals examined.

Diploid strains with mutations in *MLH1* or *PMS1* have reduced spore viability compared to wild-type strains, with *mlh1* alleles having a stronger effect than *pms1* alleles (Prolla *et al.* 1994; Hunter and Borts 1997; Wang *et al.* 1999). Compared to the wild-type strain (84% spore viability), we found significant ($P < 0.0001$) decreases in total spore viability with the *mlh1*Δ, *pms1*Δ, and *mlh1-E31A* strains (69, 77, and 79% spore viabilities, respectively), but not with the *pms1-E61A* strain (84% spore viability; $P = 0.2$). There also were significant ($P < 0.01$) elevations in the proportion of tetrads with two viable and two inviable spores for the *mlh1*Δ, *pms1*Δ, and *mlh1-E31A* strains but not for the *pms1-E61A* strain; none of the MMR-deficient strains had a significant elevation in the proportion of tetrads with three viable spores (Figure 4). The *mlh1*Δ and *mlh1-E31A* strains were significantly different from each other in all spore viability classes except the class with three viable spores.

The specific increase in the proportion of tetrads with two live:two dead spores is consistent with either meiosis I nondisjunction resulting from reduced crossing over or segregation of a heterozygous recessive lethal muta-

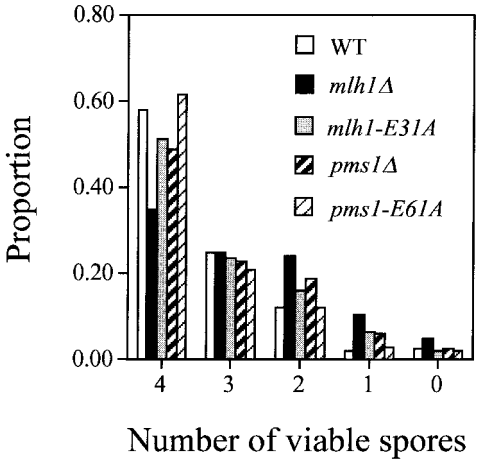

FIGURE 4.—Spore viability patterns in wild-type and mutant strains. The proportions of tetrad classes are based on the analysis of 1074 (wild type), 1005 (*mlh1*Δ), 931 (*mlh1-E31A*), 975 (*pms1*Δ), and 696 (*pms1-E61A*) tetrads. All diploids were sporulated without prior purification (see MATERIALS AND METHODS).

tion. Meiosis I nondisjunction involving chromosome *III* can be readily assessed, with the two surviving spores predicted to be nonmaters because of heterozygosity at *MAT*. WANG *et al.* (1999) reported that 20 of 1632 tetrads in an *mlh1*Δ deletion strain had this segregation pattern, whereas no such tetrads were observed in wild-type or *pms1*Δ strains. Among the 1936 tetrads derived from the *mlh1*Δ and *mlh1-E31A* homozygous strains examined here, we found only 3 with the pattern of two nonmating spores and two dead spores. PCR analysis with *MAT***a**- and *MAT*α-specific primers indicated that only 1 of the tetrads contained spores disomic for chromosome *III* (data not shown). In samples of 1074, 975, and 696 tetrads from wild-type, *pms1*Δ, and *pms1-E61A* strains, respectively, none had the segregation pattern characteristic of meiosis I nondisjunction of chromosome *III*. These results suggest that, although the *mlh1*Δ mutation clearly reduces the frequency of crossing over on chromosome *III*, this reduction is not sufficient to result in elevated meiosis I nondisjunction. The difference between our results and those of WANG *et al.* (1999) may reflect the different genetic backgrounds used in the two studies; in our genetic background, the *HIS4* locus (on chromosome *III*) is an extraordinarily strong recombination hotspot (WHITE *et al.* 1993). In addition, in our experiments, the strains were sporulated at 18° rather than at room temperature.

Different efficiencies of mismatch repair in different strain backgrounds: As described above, the *pms1-E61A* allele had no significant effect on mutation rates at the *CAN1* locus in the haploid strain SJR1392 (Table 2), while the *mlh1-E31A* allele resulted in a mutator phenotype intermediate between those of wild-type and *mlh1*Δ strains (Table 3). Because these mutator assays were done in a strain background unrelated to the strains

TABLE 6

Forward mutation rate at the *CAN1* locus in AS4- and PD73-related haploids

Strain	Relevant genotype	*CAN1* mutation rate ($\times 10^{-7}$)[a]	Fold increase in rate[b]
PD73 derivatives			
PD73	Wild type	1.2 (1.1–1.7)	1
HMY91	*mlh1*Δ*::kanMX4*	17 (15–24)	14
JSY88	*mlh1-E31A*	11 (8–17)	9
HMY92	*pms1*Δ*::kanMX4*	16 (13–23)	13
JSY116	*pms1-E61A*	2.3 (2.1–2.7)	2
AS4 derivatives			
JSY106	Wild type	0.9 (0.6–1.1)	1
JSY108	*mlh1*Δ*::URA3*	20 (17–25)	23
JSY104	*mlh1-E31A*	21 (19–28)	25
JSY107	*pms1*Δ	35 (28–48)	41
JSY105	*pms1-E61A*	2 (1.1–5.8)	2

[a] Rates were calculated by fluctuation analysis as described in MATERIALS AND METHODS. Numbers in parentheses indicate 95% confidence intervals.

[b] The rates observed for the mutant strains were divided by the wild-type rate.

used in the meiotic experiments, we repeated the *CAN1* mutator assay in derivatives of the haploid parental strains used to construct the diploids (Table 6). In agreement with earlier studies (TRAN and LISKAY 2000) and the results reported here with the SJR1392 derivatives, the effect of the *mlh1-E31A* allele is about one-half that observed in the *mlh1*Δ mutant, whereas the effect of *pms1-E61A* on mutation rate is very subtle. Although the mutator phenotypes reported here are qualitatively similar in different strain backgrounds, the absolute effects of null mutations in *MLH1* and *PMS1* on the forward mutation rate at the *CAN1* locus vary considerably between strains. Relative to the isogenic wild-type strain, deletion of *MLH1* or *PMS1* elevates the *CAN1* mutation rate ~60-fold in the SJR1392 background (Tables 2 and 3), 30-fold in the AS4 background, and only 15-fold in the PD73 background (Table 6). Although rate differences of this sort generally are attributed to minor variations in the mutator assay as performed in different labs at different times, the mutator phenotypes for AS4 and PD73 were determined simultaneously. In addition, we performed side-by-side *CAN1* mutation rate measurements for SJR1392 and PD73 and confirmed that the mutation rates are elevated to different extents in *mlh1*Δ mutants (data not shown). The strain-to-strain differences in mutation rates documented here likely reflect strain-dependent differences in the fidelity of DNA polymerase and/or differences in the efficiency of MMR.

DISCUSSION

Although the precise roles of MutL homologs are not known, it is generally assumed that heterodimers of

these proteins serve as "matchmakers" to couple MutS-dependent mismatch recognition to the appropriate processing steps (see Harfe and Jinks-Robertson 2000a). The nature of the downstream processing steps is not clear, however, nor is it known whether these steps are identical in all MMR-related processes. For example, the repair of mismatch-containing replication intermediates must incorporate a strand discrimination step, which may not be relevant to the recognition/repair of mismatches in recombination intermediates. To address possible dissimilarities between MMR mechanisms in replication *vs.* recombination, we randomly mutagenized the *PMS1* gene and screened for alleles that differentially affected the mitotic spellchecker and antirecombination activities of the corresponding proteins. Two such separation-of-function alleles were identified in the screen (*pms1-L124S* and *pms1-I854M*), each of which resulted in a reduction in the antirecombination activity of Pms1p, but had no significant effect on the spellchecker function. When the *pms1-I854M* mutation was combined in the same gene with mutations similar to the *pms1-L124S* mutation (*pms1-E61A,I854M* and *pms1-G128A,I854M* double-mutant alleles; Table 2), the mutations were not epistatic and, therefore, likely affect the function of the Mlh1p-Pms1p complex in fundamentally different ways.

The alteration conferred by the *pms1-I854M* allele is within the C-terminal 200 amino acids of Pms1p, a region that is highly conserved with the human PMS2 protein, but is not represented in the yeast and human Mlh1 proteins or in the bacterial MutL protein (Crouse 1998). Because the conserved C-terminal region of Pms1p is required for ATP-independent heterodimer formation with Mlh1p (Pang *et al.* 1997), the separation-of-function phenotype associated with the *pms1-I854M* allele might simply reflect a reduction in the amount of the Mlh1p-Pms1p complex, with full antirecombination activity requiring more of the complex than the spellchecker function. Our two-hybrid analysis (Figure 3) indicates, however, that the I854M amino acid change does not significantly affect the level of the Mlh1p-Pms1p interaction. An alternative to a stability-related explanation for the *pms1-I854M* separation-of-function phenotype derives from studies of the C-terminal region of the bacterial MutL protein, which not only is important for analogous homodimer formation (Drotschmann *et al.* 1998), but also is required for interaction of MutL with the MutH endonuclease and with the UvrD helicase in two-hybrid assays (Hall *et al.* 1998; Hall and Matson 1999). It thus is intriguing to speculate that the *pms1-I854M* mutation alters an interaction with a protein that is important in mitotic antirecombination, but that plays little, if any, role in mutation avoidance. Candidates for such a protein might include members of the *RAD52* epistasis group of recombination proteins (Sung *et al.* 2000) if mismatches are sensed during the strand invasion process or might include proteins involved in disrupting or destroying a recombination intermediate (*e.g.*, helicases or nucleases) if mismatches are detected after formation of stable heteroduplex DNA.

Although it is unclear how the *pms1-I854M* mutation impacts protein function, the *pms1-L124S* allele changes an amino acid that is immediately adjacent to conserved motif III of the GLH superfamily of ATPases (Figure 2). Motif III is part of the "ATP lid," which undergoes dramatic conformational change when the N-terminal fragment of MutL (LN40) binds ATP (Ban *et al.* 1999). This ATP-dependent conformational change is accompanied by dimerization of LN40, which is required for subsequent ATP hydrolysis and is speculated to be critical for the interaction of MutL with proteins that participate in the downstream steps of MMR. The weak ATPase activity of MutL presumably returns the protein to its starting conformation so that it can participate in another round of MMR. The situation is more complex in eukaryotes than in bacteria, with the active forms of the comparable MutL-like complexes being heterodimers. A functional asymmetry in the yeast Mlh1p-Pms1p heterodimer has been observed in genetic studies in which targeted mutations were introduced into the ATP binding/hydrolysis domains of the individual subunits (Tran and Liskay 2000). In these studies, mutations that impacted ATP binding or the associated conformational changes (*mlh1-G98A* and *pms1-G128*) resulted in a stronger mutator phenotype than that of the ATP hydrolysis mutations (*mlh1-E31A* and *pms1-E61A*), and the mutations in Mlh1p resulted in a stronger mutator phenotype than that of the comparable mutations in Pms1p (Tran and Liskay 2000). On the basis of these results, it was suggested that ATP binding by the individual subunits in the Mlh1p-Pms1p complex may be sequential, with ATP binding by Mlh1p preceding and perhaps facilitating ATP binding/hydrolysis by Pms1p. In support of this model, recent biochemical studies have shown that an N-terminal fragment of yeast Mlh1p binds ATP with 10-fold higher affinity than does a comparable N-terminal fragment of Pms1p (Hall *et al.* 2002; see also Tomer *et al.* 2002). The asymmetry between Mlh1p and Pms1p may not be limited only to ATP binding, but may also extend to ATP hydrolysis, as each N-terminal fragment has inherent ATPase activity (Guarne *et al.* 2001; Hall *et al.* 2002). This is in contrast to an N-terminal fragment of the bacterial MutL protein, where only the homodimer exhibits ATPase activity (Ban *et al.* 1999).

According to the model described above, the Mlh1p-Pms1p complex would be expected to retain some function if the ATPase activity of Pms1p is compromised, but would be expected to retain little, if any, function if the ATPase activity of Mlh1p is eliminated. This prediction not only is consistent with spellchecker phenotypes reported previously (Tran and Liskay 2000), but

also is supported by the recombination analyses reported here, with mutations in the ATPase domain of Mlh1p resulting in a more severe *in vivo* phenotype than those in the ATPase domain of Pms1p. The functional asymmetry observed for the ATPase domains of Mlh1p and Pms1p in correcting DNA replication errors (Tran and Liskay 2000) thus extends to the mitotic antirecombination function of the MMR system as well as to the repair of mismatches in meiotic recombination intermediates.

In addition to the asymmetry between Mlh1p and Pms1p observed in both the spellchecker and recombination assays, the results reported here indicate that disruption of the ATPase activity of Pms1p impacts the recombination-related functions of the Mlh1p-Pms1p complex more than the replication-related spellchecker function. The differential effect was evident when examining mitotic recombination between homeologous substrates (Table 2) and when assessing the repair of mismatches in meiotic recombination intermediates (Table 4). These results suggest that the cycles of conformational changes induced by ATP binding/hydrolysis by Pms1p are more important in the recognition or processing of DNA mismatches in recombination intermediates than in the recognition or processing of DNA mismatches resulting from DNA replication errors. Although the purpose of these conformational changes is not clear, it is likely that they are important in interactions of the Mlh1p-Pms1p heterodimer with other proteins involved in MMR-related functions. The proteins required for processing mismatch-containing recombination *vs.* replication intermediates may be different or the proteins simply could be present at different levels in recombination *vs.* replication intermediates. For example, proliferating cell nuclear antigen (PCNA), which is known to interact with MMR proteins (Johnson *et al.* 1996a; Umar *et al.* 1996; Flores-Rozas *et al.* 2000), would be expected to be found at high concentrations at DNA replication forks, but may not necessarily be present at high levels in a heteroduplex recombination intermediate. Thus, the Pms1p ATPase motifs might be necessary for formation and/or stability of a functional mismatch-repair complex in the absence of PCNA. Alternatively, the ATPase activity of Pms1p may be required to direct the activity of downstream factors in the absence of a replication-associated signal that determines which strand is to be repaired.

Although we favor the explanation that the *pms1-E61A*, *pms1-L124S*, and *pms1-G128A* mutations partially separate the functions of the yeast Mlh1p-Pms1p complex in replication and recombination, there are several caveats to this conclusion. First, since the assays used to monitor recombination-related functions of the MMR system were quite different from those used to assess the spellchecker function, we cannot rule out the possibility of DNA sequence-specific or chromosome context-specific effects on MMR activity. In addition, there may be competing systems of repair that operate differently on recombination *vs.* replication intermediates. Finally, recombination-related processes may be more sensitive to the concentration of the Mlh1p-Pms1p complex than are replication-related processes. It is formally possible that the separation-of-function mutations in *PMS1* decrease the overall stability of the protein and thereby reduce the concentration of the Mlh1p-Pms1p complex. Such a stability explanation has been invoked to explain *MLH1* separation-of-function alleles that affect the repair of mismatches in meiotic recombination intermediates more than meiotic crossing over (Argueso *et al.* 2002). Although we have not directly examined the stabilities of the mutant Pms1p proteins, as reported here for the *pms1-I854M* allele, introduction of the *PMS1* or *MLH1* ATP binding/hydrolysis mutations does not affect the stability of two-hybrid fusion proteins (Tran and Liskay 2000).

In summary, the results presented here demonstrate that it is possible to mutationally separate the replication *vs.* recombination roles of the yeast Pms1p protein. The identification of *pms1* separation-of-function alleles is consistent with the notion that the Mlh1p-Pms1p complex couples mismatch recognition to the appropriate downstream processing steps and suggests that the downstream steps may differ, depending on the context of the mismatch. A major goal of future MMR studies in yeast will be to define the relevant downstream steps in replication *vs.* recombination processes.

We thank D. Brenner for help with the genetic analysis. This work was supported by National Institutes of Health (NIH) grants GM-24110 to T.D.P., GM-38464 to S.J.-R., and GM-45413 to R.M.L. P.T.T. was supported by NIH training grant HL-07781; J.S. and H.M.K. were supported by NIH training grant GM-07092.

LITERATURE CITED

Ali, J. A., A. P. Jackson, A. J. Howells and A. Maxwell, 1993 The 43-kilodalton N-terminal fragment of the DNA gyrase B protein hydrolyzes ATP and binds coumarin drugs. Biochemistry **32:** 2717–2724.

Argueso, J. L., D. Smith, J. Yi, M. Waase, S. Sarin *et al.*, 2002 Analysis of conditional mutations in the *Saccharomyces cerevisiae MLH1* gene in mismatch repair and in meiotic crossing over. Genetics **160:** 909–921.

Ban, C., and W. Yang, 1998 Crystal structure and ATPase activity of MutL: implications for DNA repair and mutagenesis. Cell **95:** 541–552.

Ban, C., M. Junop and W. Yang, 1999 Transformation of MutL by ATP binding and hydrolysis: a switch in DNA mismatch repair. Cell **97:** 85–97.

Bartel, P., C. T. Chien, R. Sternglanz and S. Fields, 1993 Elimination of false positives that arise in using the two-hybrid system. Biotechniques **14:** 920–924.

Bartsch, S., L. E. Kang and L. S. Symington, 2000 *RAD51* is required for the repair of plasmid double-stranded DNA gaps from either plasmid or chromosomal templates. Mol. Cell. Biol. **20:** 1194–1205.

Boeke, J. D., F. LaCroute and G. R. Fink, 1984 A positive selection for mutants lacking orotidine-5′-phosphate decarboxylase activity in yeast: 5-fluoro-orotic acid resistance. Mol. Gen. Genet. **197:** 345–346.

Chen, W., and S. Jinks-Robertson, 1998 Mismatch repair proteins regulate heteroduplex formation during mitotic recombination in yeast. Mol. Cell. Biol. **18:** 6525–6537.

Chen, W., and S. Jinks-Robertson, 1999 The role of the mismatch repair machinery in regulating mitotic and meiotic recombination between diverged sequences in yeast. Genetics **151:** 1299–1313.

Crouse, G. F., 1998 Mismatch repair systems in *Saccharomyces cerevisiae*, pp. 411–448 in *DNA Damage and Repair, Volume 1: DNA Repair in Prokaryotes and Lower Eukaryotes*, edited by J. A. Nickoloff and M. F. Hoekstra. Humana Press, Totowa, NJ.

Datta, A., A. Adjiri, L. New, G. F. Crouse and S. Jinks-Robertson, 1996 Mitotic crossovers between diverged sequences are regulated by mismatch repair proteins in *Saccharomyces cerevisiae*. Mol. Cell. Biol. **16:** 1085–1093.

Datta, A., M. Hendrix, M. Lipsitch and S. Jinks-Robertson, 1997 Dual roles for DNA sequence identity and the mismatch repair system in the regulation of mitotic crossing-over in yeast. Proc. Natl. Acad. Sci. USA **94:** 9757–9762.

Detloff, P., J. Sieber and T. D. Petes, 1991 Repair of specific base pair mismatches formed during meiotic recombination in the yeast *Saccharomyces cerevisiae*. Mol. Cell. Biol. **11:** 737–745.

Dixon, W. J., and F. J. Massey, Jr., 1969 *Introduction to Statistical Analysis*. McGraw-Hill, New York.

Drotschmann, K., A. Aronshtam, H.-J. Fritz and M. G. Marinus, 1998 The *Escherichia coli* MutL protein stimulates binding of Vsr and MutS to heteroduplex DNA. Nucleic Acids Res. **26:** 948–953.

Dutta, R., and M. Inouye, 2000 GHKL, an emergent ATPase/kinase superfamily. Trends Biochem. Sci. **25:** 24–28.

Fan, Q., F. Xu and T. D. Petes, 1995 Meiosis-specific double-strand DNA breaks at the *HIS4* recombination hot spot in the yeast *Saccharomyces cerevisiae*: control in *cis* and *trans*. Mol. Cell. Biol. **15:** 1679–1688.

Fleig, U. N., R. D. Pridmore and P. Philippsen, 1986 Construction of *LYS2* cartridges for use in genetic manipulations of *Saccharomyces cerevisiae*. Gene **46:** 237–245.

Flores-Rozas, H., and R. D. Kolodner, 1998 The *Saccharomyces cerevisiae MLH3* gene functions in *MSH3*-dependent suppression of frameshift mutations. Proc. Natl. Acad. Sci. USA **95:** 12404–12409.

Flores-Rozas, H., D. Clark and R. D. Kolodner, 2000 Proliferating cell nuclear antigen and Msh2p-Msh6p interact to form an active mispair recognition complex. Nat. Genet. **26:** 375–378.

Fogel, S., R. Mortimer, K. Lusnak and F. Tavares, 1979 Meiotic gene conversion: a signal of the basic recombination event in yeast. Cold Spring Harbor Symp. Quant. Biol. **43:** 1325–1341.

Grenert, J. P., B. D. Johnson and D. O. Toft, 1999 The importance of ATP binding and hydrolysis by hsp90 in formation and function of protein heterocomplexes. J. Biol. Chem. **274:** 17525–17533.

Guarne, A., M. S. Junop and W. Yang, 2001 Structure and function of the N-terminal 40 kDa fragment of human PMS2: a monomeric GHL ATPase. EMBO J. **20:** 5521–5531.

Hall, M., and S. W. Matson, 1999 The *Escherichia coli* MutL protein physically interacts with MutH and stimulates the MutH-associated endonuclease activity. J. Biol. Chem. **274:** 1306–1312.

Hall, M. C., J. R. Jordan and S. W. Matson, 1998 Evidence for a physical interaction between the *Escherichia coli* methyl-directed mismatch repair proteins MutL and UvrD. EMBO J. **17:** 1535–1541.

Hall, M. C., P. V. Shcherbakova and T. A. Kunkel, 2002 Differential ATP binding and intrinsic ATP hydrolysis by amino-terminal domains of the yeast Mlh1 and Pms1 proteins. J. Biol. Chem. **277:** 3673–3679.

Harfe, B. D., and S. Jinks-Robertson, 2000a DNA mismatch repair and genetic instability. Annu. Rev. Genet. **34:** 359–399.

Harfe, B. D., and S. Jinks-Robertson, 2000b Mismatch repair proteins and mitotic genome stability. Mutat. Res. **451:** 151–167.

Harfe, B. D., B. K. Minesinger and S. Jinks-Robertson, 2000 Discrete in vivo roles for the MutL homologs Mlh2p and Mlh3p in the removal of frameshift intermediates in budding yeast. Curr. Biol. **10:** 145–148.

Hunter, N., and R. H. Borts, 1997 Mlh1 is unique among mismatch repair proteins in its ability to promote crossing-over during meiosis. Genes Dev. **11:** 1573–1582.

Johnson, R. E., G. K. Kivvali, S. N. Guzder, N. S. Amin, C. Holm *et al.*, 1996a Evidence for involvement of yeast proliferating cell nuclear antigen in DNA mismatch repair. J. Biol. Chem. **271:** 27987–27990.

Johnson, R. E., G. K. Kovvali, L. Prakash and S. Prakash, 1996b Requirement of the yeast *MSH3* and *MSH6* genes for *MSH2*-dependent genomic stability. J. Biol. Chem. **271:** 7285–7288.

Kramer, W., B. Kramer, M. S. Williamson and S. Fogel, 1989 Cloning and nucleotide sequence of DNA mismatch repair gene *PMS1* from *Saccharomyces cerevisiae*: homology of PMS1 to procaryotic MutL and HexB. J. Bacteriol. **171:** 5339–5346.

Lamers, M. H., A. Perrakis, J. H. Enzlin, H. H. K. Winterwerp, N. de Wind *et al.*, 2000 The crystal structure of DNA mismatch repair protein MutS binding to a G:T mismatch. Nature **407:** 711–717.

Lea, D. E., and C. A. Coulson, 1949 The distribution of the numbers of mutants in bacterial populations. J. Genet. **49:** 264–285.

Longtime, M. S., A. McKenzie, III, D. J. Demarini, N. G. Shah, A. Wach *et al.*, 1998 Additional modules for versatile and economical PCR-based gene deletion and modification in *Saccharomyces cerevisiae*. Yeast **14:** 953–961.

Marsischky, G. T., N. Filosi, M. F. Kane and R. Kolodner, 1996 Redundancy of *Saccharomyces cerevisiae MSH3* and *MSH6* in *MSH2*-dependent mismatch repair. Genes Dev. **10:** 407–420.

Modrich, P., and R. Lahue, 1996 Mismatch repair in replication fidelity, genetic recombination and cancer biology. Annu. Rev. Biochem. **65:** 101–133.

Muhlrad, D., R. Hunter and R. Parker, 1992 A rapid method for localized mutagenesis of yeast genes. Yeast **8:** 79–82.

Myung, K., A. Datta, C. Chen and R. D. Kolodner, 2001 SGS1, the Saccharomyces cerevisiae homologue of BLM and WRN, suppresses genome instability and homeologous recombination. Nat. Genet. **27:** 1–4.

Nag, D. K., M. A. White and T. D. Petes, 1989 Palindromic sequences in heteroduplex DNA inhibit mismatch repair in yeast. Nature **340:** 318–320.

Nicholson, A., M. Hendrix, S. Jinks-Robertson and G. F. Crouse, 2000 Regulation of mitotic homeologous recombination in yeast: functions of mismatch repair and nucleotide excision repair genes. Genetics **154:** 133–146.

Obmolova, G., C. Ban, P. Hsieh and W. Yang, 2000 Crystal structures of mismatch repair protein MutS and its complex with a substrate DNA. Nature **407:** 703–710.

Pang, Q., T. A. Prolla and R. M. Liskay, 1997 Functional domains of the *Saccharomyces cerevisiae* Mlh1p and Pms1p DNA mismatch repair proteins and their relevance to human hereditary nonpolyposis colorectal cancer-associated mutations. Mol. Cell. Biol. **17:** 4465–4473.

Perkins, D. D., 1949 Biochemical mutants in the smut fungus *Ustilago maydis*. Genetics **34:** 607–626.

Petes, T. D., R. E. Malone and L. S. Symington, 1991 Recombination in yeast, pp. 407–521 in *The Molecular Biology of the Yeast Saccharomyces: Genome Dynamics, Protein Synthesis and Energetics*, edited by J. R. Broach, J. R. Pringle and E. W. Jones. Cold Spring Harbor Laboratory Press, Cold Spring Harbor, NY.

Prodromou, C., S. M. Roe, R. O'Brien, J. E. Ladbury, P. W. Piper *et al.*, 1997a Identification and structural characterization of the ATP/ADP-binding site in the Hsp90 molecular chaperone. Cell **90:** 65–75.

Prodromou, C., S. M. Roe, P. W. Piper and L. H. Pearl, 1997b A molecular clamp in the crystal structure of the N-terminal domain of the yeast Hsp90 chaperone. Nat. Struct. Biol. **4:** 477–482.

Prolla, T. A., D.-M. Christie and R. M. Liskay, 1994 Dual requirement in yeast DNA mismatch repair for *MLH1* and *PMS1*, two homologs of the bacterial *mutL* gene. Mol. Cell. Biol. **14:** 407–415.

Sherman, F., 1991 Getting started with yeast. Methods Enzymol. **194:** 3–20.

Sherman, F., and P. Wakem, 1991 Mapping yeast genes. Methods Enzymol. **194:** 38–57.

Sikorski, R. S., and P. Hieter, 1989 A system of shuttle vectors and yeast host strains designed for efficient manipulation of DNA in *Saccharomyces cerevisiae*. Genetics **122:** 19–27.

Stapleton, A., and T. D. Petes, 1991 The Tn3 β-lactamase gene acts as a hotspot for meiotic recombination in yeast. Genetics **127:** 39–51.

Sung, P., K. M. Trujillo and S. Van Komen, 2000 Recombination factors of *Saccharomyces cerevisiae*. Mutat. Res. **451:** 257–275.

Tomer, G., A. B. Buermeyer, M. M. Nguyen and R. M. Liskay, 2002 Contribution of human Mlh1 and Pms2 ATPase activities to DNA mismatch repair. J. Biol. Chem. **277:** 21801–21809.

Tran, P. T., and M. Liskay, 2000 Functional studies on the candidate ATPase domains of *Saccharomyces cerevisiae* MutLα. Mol. Cell. Biol. **20:** 6390–6398.

Umar, A., A. B. Buermeyer, J. A. Simon, D. C. Thomas, A. B. Clark *et al.*, 1996 Requirement for PCNA in DNA mismatch repair at a step preceding DNA resynthesis. Cell **87:** 65–73.

Vojtek, A. B., S. M. Hollenberg and J. A. Cooper, 1993 Mammalian Ras interacts directly with the serine/threonine kinase Raf. Cell **74:** 205–214.

Wach, A., A. Brachat, R. Pohlmann and P. Philippsen, 1994 New heterologous modules for classical or PCR-based gene disruption in *Saccharomyces cerevisiae*. Yeast **10:** 1793–1808.

Wang, T.-F., N. Kleckner and N. Hunter, 1999 Functional specificity of MutL homologs in yeast: evidence for three Mlh1-based heterocomplexes with distinct roles during meiosis in recombination and mismatch correction. Proc. Natl. Acad. Sci. USA **96:** 13914–13919.

White, M. A., M. Dominska and T. D. Petes, 1993 Transcription factors are required for the meiotic recombination hotspot at the *HIS4* locus in *Saccharomyces cerevisiae*. Proc. Natl. Acad. Sci. USA **90:** 6621–6625.

Wigley, D. B., G. J. Davies, E. J. Dodson, A. Maxwell and G. Dodson, 1991 Crystal structure of an N-terminal fragment of the DNA gyrase B protein. Nature **351:** 624–629.

Williamson, M. S., J. C. Game and S. Fogel, 1985 Meiotic gene conversion mutants in *Saccharomyces cerevisiae*. I. Isolation and characterization of *pms1-1* and *pms1-2*. Genetics **110:** 609–646.

Communicating editor: A. Nicolas